

## Inelastic X-Ray Scattering from Copper *K*-Shell Electrons at Intermediate Momentum Transfers

Vincent Marchetti and Carl Franck

*Laboratory of Atomic and Solid State Physics and Materials Science Center,  
Cornell University, Ithaca, New York 14853*

(Received 19 May 1987)

We give experimental spectra for 70- and 62-keV x rays inelastically scattered from the *K*-shell electrons of copper. The x rays scattered from the *K* shell were selected by fluorescence coincidence. The scattering is in a momentum-transfer regime in which the impulse approximation is not valid, and atomic binding effects are important. The data are in agreement within experimental uncertainties in absolute scattering strength and spectra shape with a Hartree-Fock-Slater calculation. In contrast to previous work we do not see separate spectral features attributable to Compton and Raman scattering.

PACS numbers: 32.80.Cy, 32.80.Hd

At high momentum transfers inelastic x-ray scattering is well described by the impulse approximation<sup>1</sup> in which the spectrum of scattered x rays is determined by the momentum distribution of the electronic initial state. The aim of this work was to examine the x-ray scattering process beyond the impulse-approximation regime by inelastically scattering x-rays from deeply bound *K*-shell electrons of orbital radius *a* at intermediate momentum transfers ( $q_0 \lesssim 1/a$ ).<sup>2</sup> In this momentum-transfer regime, unlike the limit  $q_0 a \gg 1$ , the electron is excited to a state which is not well described as a free-electron plane wave. Furthermore, we are sensitive to electric-dipole-forbidden transitions, which are not revealed in x-ray photoabsorption spectroscopy (which is spectroscopically equivalent to the limit  $qa \ll 1$  of inelastic scattering).<sup>3</sup> We eliminate inelastic scattering from outer-shell electrons by detecting scattered x rays in coincidence with *K*-fluorescence x rays.

Previous measurements have studied the breakdown of the impulse approximation in scattering from *K*-shell electrons of Cu and Fe<sup>4,5</sup> and Ge.<sup>6</sup> The work on Cu and Fe by Namikawa and Hosoya<sup>5</sup> at  $q_0 a \approx 1.0$ , which motivated this work, indicated the existence of two features in the scattering spectrum: A "Raman" peak at small energy transfer and a separate "Compton" feature of roughly equal magnitude at large energy transfer. We show that such a splitting of the scattered x-ray spectrum would contradict a standard one-electron description of x-ray scattering from a bound electron. Our measurements, which cover a range of momentum transfers  $0.53 \leq q_0 a \leq 1.11$ , do not show the separate Compton feature at high energy transfers, in agreement with the one-electron model. Manninen<sup>7</sup> has criticized the previous experimental results on the basis of possible false coincidences.

This scattering experiment was performed on the A2 line at the Cornell High Energy Synchrotron Source. The incident beam, at energy  $E_0 = 70$  or 62 keV, was obtained from wiggler radiation selected by a Si(400) double crystal monochromator tuned to a fundamental energy of 35 or 31 keV. A Cu filter attenuated the funda-

mental component by a factor of 300 relative to the second harmonic. The flux in the second harmonic was estimated at  $\approx 10^8$  photons/sec. The energy bandwidth was less than the resolution of the scattered-photon detector.

Two energy-resolving detectors viewed a 7.7- $\mu\text{m}$  Cu foil target. The *K*-fluorescence detector, a Si(Li) detector with an energy resolution of 420 eV at 8.0 keV, was located in the horizontal plane defined by the beam direction and beam polarization, at a 90° angle to the incident-beam direction. The active area of this detector subtended  $\approx 0.1$  sr as seen by the sample. The scattered-photon detector, an intrinsic Ge detector with an energy resolution of 500 eV at 81 keV, was set at the scattering angle  $\theta$  in the vertical plane. This detector subtended  $\approx 2.8 \times 10^{-2}$  sr. The sample was oriented differently for each scattering angle such that the incident angle of the x-ray beam on the sample varied between 38° and 53° from perpendicular. The exit angle for fluorescence x rays was a constant 60°, and the exit angle for scattered x rays varied between 34° and 54°. The scattered x rays were seen in transmission geometry through the sample for the lowest two scattering angles and in reflection geometry from the sample for the highest two scattering angles. The counting rates were on the order of 5000 sec<sup>-1</sup> in the Si(Li) detector and 1500 sec<sup>-1</sup> in the Ge detector.

A fast-slow coincidence system<sup>8</sup> allowed the recording of the energy of scattered x rays. This system sent a gating pulse to a pulse-height analyzer upon the detection of a signal in both detectors during a single synchrotron pulse and a signal in the Si(Li) detector corresponding to an x ray in the *K*-fluorescence energy window 7.4 to 9.5 keV. Only scattered x rays with energy above  $\approx 28$  keV were counted. The coincidence events arise from truly correlated events, i.e., an event in which a single incident x ray causes the emission of two x rays; and from uncorrelated events, those arising from separate single-photon processes such as the scattering of one incident x ray and a fluorescence decay following photoabsorption of another incident x ray. To eliminate accidental counts

caused by uncorrelated events, we measured for equal amounts of time in a coincidence mode, in which the two detectors were compared on a single x-ray pulse, and in a mode we call the acoincidence mode, in which the signal from the scattered x-ray detector was delayed by the period of synchrotron pulses,  $\approx 360$  nsec. This time is equivalent to the time resolution in our coincidence detection, and is larger than the time resolution of 60 nsec<sup>5</sup> possible with continuous sources. This limitation partially offsets the advantage of high beam intensity. The spectra presented in Fig. 1 are the difference between the spectra recorded in coincidence mode and in acoincidence mode. The rate of accidental coincidences was proportional to the square of incident intensity while the rate of true events was proportional to intensity, and so it was necessary to switch between detection modes with a period short enough that the intensity was essentially constant over a joint measurement in both modes. For the spectra shown here, the modes were switched with a period of either 8 or 16 sec. A typical spectrum,

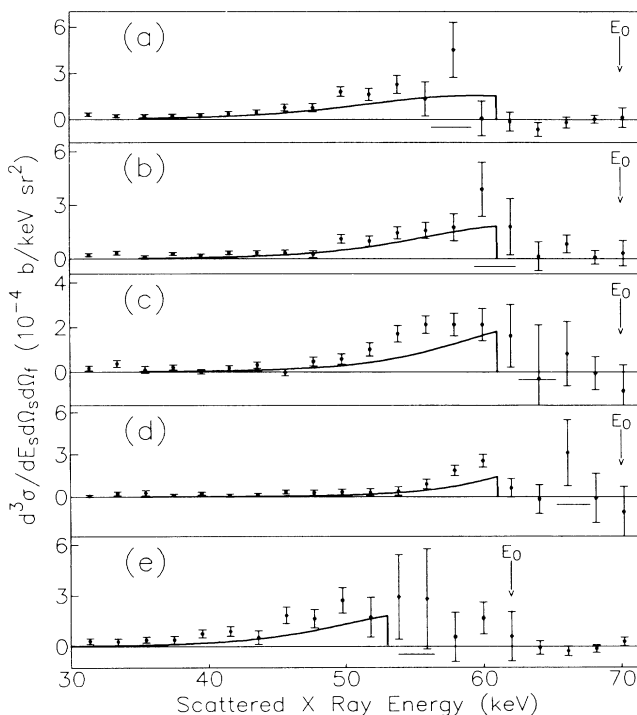


FIG. 1. Spectra of x rays inelastically scattered from copper  $K$ -shell electrons. Scattering is at incident energy  $E_0$ , scattering angle  $\theta$ , and scaled momentum transfer (for elastic scattering)  $q_0 a$  (where  $a$  is the  $K$ -shell Bohr radius) as follows: (a)  $E_0 = 70$  keV,  $\theta = 118^\circ$ , and  $q_0 a = 1.11$ ; (b) 70 keV,  $88^\circ$ , 0.90; (c) 70 keV,  $70^\circ$ , 0.74; (d) 70 keV,  $49^\circ$ , 0.53; (e) 62 keV,  $88^\circ$ , 0.79. Experimental normalizations have an uncertainty factor of  $\pm 40\%$ , constant for all spectra. Solid curves are theoretical Hartree-Fock-Slater results. Solid line segments under base lines indicate full width at half maximum of total atomic inelastic scattering (Compton) spectra.

at  $E_0 = 70$  keV and  $\theta = 118^\circ$ , was taken over 6 h and contained 29 168 counts recorded in acoincidence mode and 30 521 counts in coincidence mode. The signal from correlated events represented  $\approx 4.6\%$  of the total number of coincidence events [and  $\approx 0.005\%$  of the number of single-scattering events, which were predominantly inelastic (Compton) scattering]. The success of the subtraction of the accidental counts from our spectra can be judged by the regions in which there should be no true coincidence scattering events, in particular the energy region above the threshold energy ( $E_0 - E_B$ , where  $E_0$  is the incident x-ray energy and  $E_B$  is the  $K$ -shell binding energy, 8.98 keV<sup>9</sup>), up to and including the incident energy.

We measure the triply differential cross section for scattering into the energy range  $dE_s$  and solid angle  $d\Omega_s$  and emission of a fluorescence x ray into the solid angle  $d\Omega_f$ . Spectra were taken at four scattering angles,  $\theta = 49^\circ, 70^\circ, 88^\circ$ , and  $118^\circ$ , at  $E_0 = 70$  keV and at a single scattering angle,  $\theta = 88^\circ$ , at  $E_0 = 62$  keV. The difference spectra are shown in Fig. 1. The data shown are the result of grouping together the counts from bins of twenty pulse-height analyzer channels. The largest errors occur in regions (indicated in Fig. 1) in which the outer-electron Compton-scattering feature falls, as the accidental rates are largest at these energies and the statistical uncertainties in the rates recorded in coincidence and acoincidence mode are greatest. This figure also includes theoretical scattering spectra to be discussed. The data were normalized independently of this theory by comparison of the rate of true coincidences to the total rate of  $K$ -shell fluorescence excited by photoabsorption. The photoabsorption cross section<sup>10</sup> at 70 keV was taken to be 86.7 b and at 62 keV was 124.5 b, and a value of 0.451 was used for the radiative yield of  $K$ -shell decay following photoabsorption.<sup>11</sup> We also took into account the absorption of Cu  $K$  x rays in the sample. The normalization factor includes a systematic error, constant for all the spectra, of  $\pm 40\%$ , due to the uncertainty in the geometric efficiency of the detectors. Except for the expected energy shift, the spectra corresponding to different incident energies [Figs. 1(b) and 1(e)] agree, as expected for inelastic scattering when the incident energy is far from an allowed transition. The cross sections for the scattering x rays are small enough<sup>10</sup> that we do not expect multiple scattering in a sample of our thickness to be an important effect.

The signal of correlated events can contain contributions from physical processes other than  $K$ -shell scattering.<sup>8</sup> A source of these false events is detector-to-detector scattering<sup>5,7</sup> (which gave a significant spectral feature in Ref. 5). In these events a single x ray scatters from the fluorescence detector into the scattered x-ray detector. The recoil energy deposited in the fluorescence detector can mimic a true fluorescence x ray. We avoided this signal by placing lead shielding between the

detectors. We checked this shielding by taking spectra with lead shielding blocking the direct path from the sample to the scattered x-ray detector. The resulting spectra were statistically consistent with there being no detector-to-detector events, and the maximum amplitude seen in these test spectra corresponded to signal of  $0.8 \times 10^{-4}$  b/keV sr<sup>2</sup> when normalized to the same total incident x-ray flux as the spectra presented in Fig. 1. Another source of correlated events is the production of fluorescence x rays by recoil electrons from inelastic x-ray scattering. This signal will only be seen for scattering events in which the recoil electron has a kinetic energy greater than the Cu binding energy. On the basis of the cross section for ionization by electron impact<sup>12</sup> and the overall rate of energy loss of the electron,<sup>13</sup> we estimate this signal in the worst case to be less than  $1 \times 10^{-6}$  b/keV sr<sup>2</sup>, an insignificant amount. Finally, bremsstrahlung emission from photoelectrons is expected to give a monotonically decreasing contribution to the apparent cross section with increasing scattered x-ray energy.<sup>14</sup> An estimate based on Refs. 13 and 14 gives an apparent rate of  $\approx 0.15 \times 10^{-4}$  b/keV sr<sup>2</sup> at 35-keV scattered en-

ergy (70-keV incident). This is consistent with the slight signal strength observed at low energies ( $< 40$  keV).

Some basic features of the spectra are presented in Fig. 2, which shows the x-ray scattering intensity summed over the scattered x-ray energy, the energy centroid of the spectrum of scattered x rays, and the width of the spectrum. The width is the square root of the normalized second moment of the spectrum. The position of the centroid is given relative to the threshold energy. The summations were performed for both the experimental and theoretical spectra between the *K*-edge threshold energy and 25 keV below the threshold. The experimental errors shown are statistical. The data for the total scattering intensity contain an additional uncertainty factor of  $1.0 \pm 0.4$  from the normalization procedure, but this factor is constant for all the data. This uncertainty is not present in either the centroid or width.

The theoretical curves shown in Fig. 1 are the results of a one-electron calculation [see Ref. 1, Eq. (6)] in the Hartree-Fock-Slater approximation with the Herman-Skillman atomic potential of Cu for the initial and final states.<sup>15</sup> Only the scattering due to the  $A^2$  term in the nonrelativistic Hamiltonian was included. Final states with angular momentum from 0 to 5 were included. We do not expect bound-state and solid-state effects to be important at this energy resolution; and the curves in Fig. 1 were carried to the threshold energy by linear extrapolation from the calculation's lower limit of 260 eV above threshold. In order to compare the theory directly with the experimental results, we adopted the simplest model for the decay of the *K*-shell hole following the scattering event. We assumed that the radiative efficiency, i.e., the ratio of radiative decay to all decay processes, is the same as that seen in decay following photoabsorption,<sup>11</sup> and that the emission of fluorescence x rays is isotropic. A previous calculation has shown that parametric (double Thomson) scattering<sup>16</sup> is weaker by 3 orders of magnitude than two-photon processes, and so it is not included here.

Data taken over a range of intermediate momentum transfers show that the inelastic scattering from the *K*-shell electrons is consistent with the one-electron model. Since the data are normalized independently of the theoretical scattering spectra, this consistency is a check of both the adequacy of the one-electron model to predict the shape of the spectrum and our assumption concerning the decay of the *K*-shell hole. The total cross sections follow the trend predicted by theory, and the centroid, a measure of the spectrum independent of normalization, is in good agreement with the theoretical results. This centroid exhibits little observable dispersion over a range in which the momentum transfer more than doubles. The width (also normalization independent) results suggest a small discrepancy between theory and experiment. This might be explained by the aforementioned bremsstrahlung emission which would, if present,

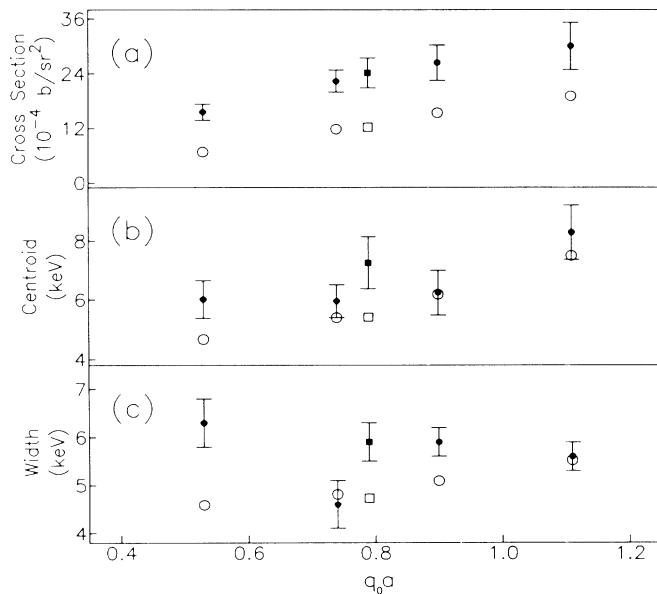


FIG. 2. Inelastic x-ray scattering cross section, centroids, and widths of spectra of inelastically scattered x rays vs scaled momentum transfer  $q_0 a$  (as for Fig. 1). Quantities calculated for region of spectrum between threshold energy (given in text) and 25 keV below threshold. (a) Cross section integrated over energy. Data normalization contains an uncertainty factor of  $1.0 \pm 0.4$  constant for all values of  $q_0 a$ . (b) Centroid of spectrum in kiloelectronvolts below threshold energy. (c) Width (square root of normalized second moment) of spectrum. Filled symbols are experimental results, open symbols results of theoretical calculation in Hartree-Fock-Slater approximation. Circles are for incident x-ray energy  $E_0 = 70$  keV, squares for  $E_0 = 62$  keV.

add strength to the apparent cross section at low scattered photon energies. This would, in turn, shift the centroid to lower energies (higher values in Fig. 2) and increase the width. In summary, our observations support the basic theoretical result that in the range of momentum transfer intermediate between that for photoabsorption ( $qa \ll 1$ ) and that for inelastic scattering in the impulse-approximation limit, the scattering length is not split into two features of approximately equal strength as reported in Ref. 5, but rather most of the scattering involves an energy transfer only  $\lesssim 5$  keV above the binding energy. This conclusion confirms some of the comments by Manninen<sup>7</sup> and contradicts a recent calculation by Ohmura and Sato<sup>17</sup> based on a more approximate one-electron model than the one presented here.

We would like to acknowledge the generous assistance of D. Bilderback, M. Bedzyk, B. Batterman, D. Mills, Xiao-lun Wu, D. Durian, D. Ripple, R. Nieminen, R. Deslattes, and J. Wilkins. We appreciate correspondence with K. Namikawa and S. Manninen and the receipt of the preprint of Y. Ohmura and S. Sato. This work was supported by the National Science Foundation through the Materials Science Center and Cornell High Energy Synchrotron Source at Cornell and by additional National Science Foundation support for one of us (V.M.).

<sup>1</sup>P. Eisenberger and P. M. Platzman, Phys. Rev. A **2**, 415

(1970).

<sup>2</sup>We define  $\hbar q_0$  as the momentum transfer in an elastic scattering:  $\hbar q_0 = 2(E_0/c) \sin(\theta/2)$ .  $E_0$  is the incident x-ray energy,  $\theta$  is the scattering angle. At fixed  $\theta$  the actual momentum transfer  $q$  varies with energy transfer. At  $\theta = 118^\circ$ ,  $q$  decreases by 23% as the energy transfer goes from 0 to 34 keV. For  $a$  we use the K-shell Bohr radius  $[(0.529 \text{ \AA})/Z]$ .

<sup>3</sup>T. Aberg and J. Tulkki, in *Atomic Inner-Shell Physics*, edited by B. Crasemann (Plenum, New York, 1985), p. 428.

<sup>4</sup>T. Fukamachi and S. Hosoya, Phys. Lett. **38A**, 341 (1972).

<sup>5</sup>K. Namikawa and S. Hosoya, Phys. Rev. Lett. **53**, 1606 (1984).

<sup>6</sup>M. Pradoux, H. Meunier, M. Avan, and G. Roche, Phys. Rev. A **16**, 2022 (1977).

<sup>7</sup>S. Manninen, Phys. Rev. Lett. **57**, 1500 (1986).

<sup>8</sup>J. Varma and M. A. Eswaran, Phys. Rev. **127**, 1197 (1962).

<sup>9</sup>J. A. Bearden and A. F. Burr, Rev. Mod. Phys. **39**, 125 (1967).

<sup>10</sup>Wm. J. Veigele, At. Data **5**, 51 (1973).

<sup>11</sup>W. Bambynek *et al.*, Rev. Mod. Phys. **44**, 716 (1972).

<sup>12</sup>C. J. Powell, Rev. Mod. Phys. **48**, 33 (1976).

<sup>13</sup>L. Pages, E. Bertel, H. Joffe, and L. Sklavenitis, At. Data **4**, 1 (1972).

<sup>14</sup>R. H. Pratt *et al.*, At. Data Nucl. Data Tables **20**, 175 (1977).

<sup>15</sup>F. Herman and S. Skillman, *Atomic Structure Calculations* (Prentice-Hall, Englewood Cliffs, NJ, 1963).

<sup>16</sup>V. Marchetti and C. Franck, Phys. Rev. A **35**, 3128 (1987).

<sup>17</sup>Y. Ohmura and S. Sato, J. Phys. Soc. Jpn. (to be published).